IEEE Photonics Journal
An IEEE Photonics Society Publication

Open Access

Deterministic Timing Jitter Analysis of SOA-Amplified Intensity-Modulated Optical Pulses

Volume 4, Number 5, October 2012

T. Alexoudi, Student Member, IEEE
G. T. Kanellos, Member, IEEE
S. Dris
D. Kalavrouziotis, Student Member, IEEE
P. Bakopoulos, Member, IEEE
A. Miliou, Member, IEEE
N. Pleros, Member, IEEE

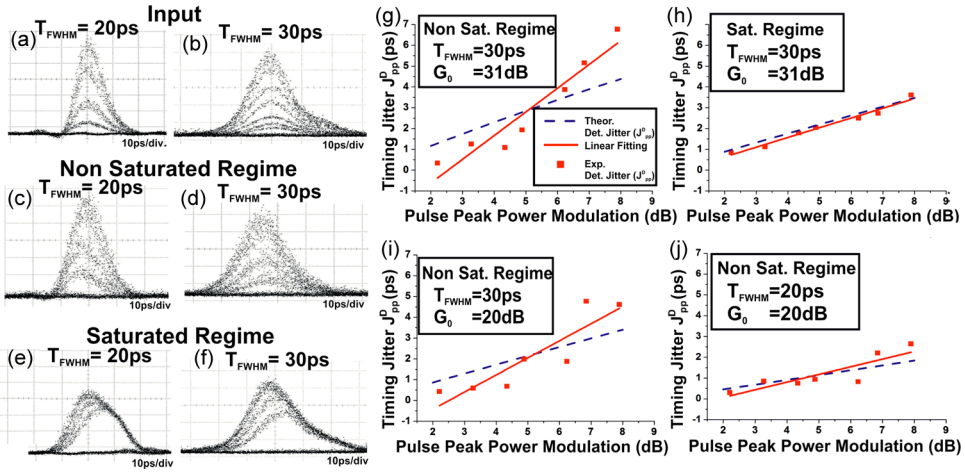

DOI: 10.1109/JPHOT.2012.2220341
1943-0655/$31.00 ©2012 IEEE

Deterministic Timing Jitter Analysis of SOA-Amplified Intensity-Modulated Optical Pulses

T. Alexoudi,[1,2] *Student Member, IEEE*, G. T. Kanellos,[2] *Member, IEEE*, S. Dris,[3] D. Kalavrouziotis,[3] *Student Member, IEEE*, P. Bakopoulos,[3] *Member, IEEE*, A. Miliou,[1] *Member, IEEE*, and N. Pleros,[1,2] *Member, IEEE*

[1]Department of Informatics, Aristotle University of Thessaloniki, 54124 Thessaloniki, Greece
[2]Center for Research and Technology Hellas, Informatics and Telematics Institute, 57001 Thessaloniki, Greece
[3]School of Electrical Engineering and Computer Engineering, National Technical University of Athens, 15780 Athens, Greece

DOI: 10.1109/JPHOT.2012.2220341

Manuscript received September 6, 2012; revised September 18, 2012; accepted September 18, 2012. Date of current version October 4, 2012. This work was supported by the European FP7 ICT-RAMPLAS (ICT- FET 270773) project. Corresponding author: T. Alexoudi (e-mail: theonial@csd.auth.gr).

Abstract: We demonstrate a detailed theoretical and experimental analysis of the deterministic timing jitter induced on intensity-modulated optical pulse streams when propagating through a SOA. The mathematical analysis reveals an approximate linear relationship between jitter and pulse intensity modulation when the SOA gain recovery time is shorter than the pulse period. The theoretical results have been confirmed by experimental deterministic timing jitter measurements for intensity modulation levels up to 8 dB, showing good agreement between theory and experiment.

Index Terms: Semiconductor optical amplifier, deterministic timing jitter, pulse peak power modulation, intensity modulation.

1. Introduction

The broad-scale efforts toward realizing high photonic integration densities has put SOA amplification in the spotlight once again, since any alternative integrated amplifier competitor [1] is far behind in terms of level of maturity. The SOA currently appears as the most preferable on-chip amplifier option in many key network subsystems, performing as pure amplifier stages [2], [3] or as ON–OFF gating elements [4] and enabling leading edge applications that extend from metro network environments [4] to access network [3] and to on-chip or on-board datacom systems [2].

The extensive application of SOAs in the photonic communications ecosystem underpins the impact of their characteristics on overall system performance. With multilevel modulation formats [5] now turning mainstream, interest in SOA amplification is further renewed. A concerted research effort on SOA-based devices spanning the last 20 years has unraveled most of their underlying amplification secrets. Pulse-shape asymmetry owing to SOA gain depletion effects, for example, has been one of the key findings and has been extensively investigated in the past [6]. However, the relationship between pulse shape distortion and timing jitter still remains a missing piece of the puzzle. Despite the detrimental effects that jitter can have on overall system performance, deterministic SOA-induced timing jitter has not been consolidated in a detailed analytical framework.

In this communication, we extend our previous work [7] and demonstrate for the first time, to the best of our knowledge, a theoretical and experimental analysis of the deterministic timing jitter induced when intensity-modulated optical pulses propagate through a SOA with a gain recovery time smaller than the pulse period. We arrive at an analytic mathematical formula for the mean pulse arrival time that provides a comprehensive picture of jitter origins, allowing for reliable prediction of the deterministic jitter induced during SOA amplification. A mathematical relationship between the deterministic jitter and the intensity modulation is derived, and the theoretical findings are verified through experiments where picosecond-long Gaussian pulses with intensity modulation depth varying from 1 to 8 dB are employed. Our analysis reveals an approximately linear relationship between deterministic timing jitter and pulse intensity modulation levels, with both experimental and theoretical results indicating that deterministic jitter minimization can be achieved by operating the SOA in the strong saturated region.

2. Deterministic Jitter Origin and Theory

It is a well-known fact that the leading edge of every incoming pulse will experience a higher gain than the trailing edge when propagating through a SOA, shifting the amplified pulse peak toward its rising edge [6]. The shift of the exiting pulse energy distribution indicates a subsequent deviation of the mean pulse arrival time T_{MEAN}. The magnitude of this timing shift is dependent on the pulse peak power, this being the root cause of the deterministic timing jitter. Specifically, when pulses of unequal peak power propagate through the SOA and assuming that the SOA gain recovers to the same steady-state value prior to the pulse arrival, the different peak power levels will generate different dips in the SOA gain, which cause different pulse shape distortions. As each pulse experiences a different amount of mean arrival time deviation, the intensity-modulated pulse stream at the output exhibits increased timing jitter values.

By defining $P_{in}(t)$ as the power of an individual incoming Gaussian pulse with peak power denoted as P_p, 1/e pulsewidth equal to T_o, and $G(t)$ as the amplifier gain experienced by this pulse, the power of the pulse exiting the amplifier is equal to $P_{out}(t) = P_{in}(t) \cdot G(t)$. The mean arrival time T_{MEAN} for every individual pulse can be calculated [8], [9] as

$$T_{MEAN} = \frac{\int_{-\infty}^{+\infty} t \cdot P_{out}(t)dt}{U_{total}} = \frac{\int_{-\infty}^{+\infty} t \cdot P_{in}(t) \cdot G(t)dt}{\int_{-\infty}^{+\infty} P_{in}(t) \cdot G(t)dt} \tag{1}$$

where U_{total} is the total output pulse energy. An analytic expression for the output power can be derived when considering the amplifier as a spatially concentrated device, with the incoming pulsewidth being much smaller than the SOA gain recovery time. This allows the use of the formula for $G(t)$ provided by Agrawal *et al.* [6]. Assuming that the pulse center is at $t = 0$ and using the respective expressions for $P_{in}(t)$ and $G(t)$ in (1), we obtain

$$\begin{aligned} T_{MEAN} &= \frac{\int_{-\infty}^{+\infty} t \cdot P_p \cdot \exp\left(-\frac{t^2}{T_o^2}\right) \cdot G(t)dt}{\int_{-\infty}^{+\infty} P_p \cdot \exp\left(-\frac{t^2}{T_o^2}\right) \cdot G(t)dt} \\ &= \frac{\int_{-\infty}^{+\infty} t \cdot P_p \cdot \exp\left(-\frac{t^2}{T_o^2}\right) \cdot \left[1 - \left(1 - \frac{1}{G_o}\right) \cdot \exp\left(\frac{-P_p \cdot \int_{-\infty}^{t} \exp\left(-\frac{t^2}{T_o^2}\right)dt}{U_{sat}}\right)\right]^{-1} dt}{\int_{-\infty}^{+\infty} P_p \cdot \exp\left(-\frac{t^2}{T_o^2}\right) \cdot \left[1 - \left(1 - \frac{1}{G_o}\right) \cdot \exp\left(\frac{-P_p \cdot \int_{-\infty}^{t} \exp\left(-\frac{t^2}{T_o^2}\right)dt}{U_{sat}}\right)\right]^{-1} dt} = \frac{A}{B} \end{aligned} \tag{2}$$

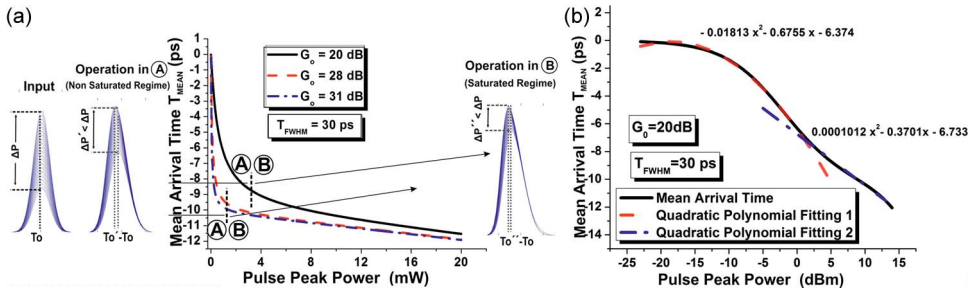

Fig. 1. (a) Theoretical mean arrival time (T_{MEAN}) versus pulse peak power values. Insets depict the schematic eye diagram of a jitter-free intensity-modulated signal prior to entering the SOA and the respective eye diagrams at the SOA output when the SOA operates in the nonsaturated (area A) and in the strongly saturated regime (area B). (b) Mean arrival time (T_{MEAN}) versus Pulse peak power expressed in dBm for $G_o = 20$ dB and 30-ps-long pulses. Dashed lines denote the fit of T_{MEAN} with second degree polynomials.

with G_o representing the steady-state gain and U_{sat} being the saturation energy parameter of the SOA. By expanding $G(t)$ both in the numerator A and in the denominator B in a first-order Taylor series around the center position of the pulse at $t = 0$, after some algebra, (2) becomes

$$T_{MEAN} = -\frac{T_o^2 \cdot \left(1 - \frac{1}{G_o}\right) \cdot \left[\frac{P_p}{U_{sat}} \cdot \exp\left(-\frac{P_p}{U_{sat}} \cdot \frac{T_o \cdot \sqrt{\pi}}{2}\right)\right]}{2 \cdot \left[1 - \left(1 - \frac{1}{G_o}\right) \cdot \exp\left(-\frac{P_p}{U_{sat}} \cdot \frac{T_o \cdot \sqrt{\pi}}{2}\right)\right]}. \tag{3}$$

Equation (3) expresses the mean arrival time of every pulse as a function of its peak power, its time duration, and the SOA steady-state gain value, and provides insight into the origin of jitter. Fig. 1(a) shows the graphical representation of T_{MEAN} versus pulse peak power for a range 0 mW to 20 mW, for three different G_o values and a 20-ps pulsewidth. Since the pulse center has been assumed at $t = 0$, the time shift induced during SOA amplification will always be leftward toward smaller values, so that T_{MEAN} is a negative quantity, continuously decreasing until reaching a saturation plateau.

Moreover, the steepness of the slope of the T_{MEAN} curve differs as the peak power level increases, so that the T_{MEAN} curve can be divided into two distinct areas: Area A, corresponding to the nonsaturated SOA gain regime, where the SOA retains sensitivity to input peak power and leads to enhanced timing jitter values for the amplified pulses, and Area B, where the SOA operates in its strongly saturated gain region. In this case, the curve of T_{MEAN} decreases smoothly, almost approaching a downward sloping tail. This effect mitigates the differences of mean arrival time compared with operation in area A and results in lower timing jitter values. At this point, we should mention that SOA operation in the nonsaturated regime corresponds to the case where the SOA gain has dropped by not more than 3 dB from its initial steady-state value, while SOA operation in its saturated region refers to the case where the SOA gain drops by more than 3 dB from its initial steady-state value upon optical pulse arrival.

The monotonic slope of mean arrival time T_{MEAN} implies that the lowest and highest values are obtained for the corresponding lowest and highest peak power input pulses. In the case of a pulse sequence with P_p values residing within a finite set between minimum and maximum values, the peak-to-peak deterministic jitter J_{pp}^D can be calculated as the difference between the respective minimum and maximum mean arrival time values T_{MEAN} as follows:

$$J_{pp}^D = T_{MEAN}^{\max} - T_{MEAN}^{\min} \tag{4}$$

where $T_{MEAN}^{\min} = T_{MEAN}(P_p^{\min})$, and $T_{MEAN}^{\max} = T_{MEAN}(P_p^{\max})$.

Fig. 1(b) is a graphical representation of (3), showing the dependence of T_{MEAN} on peak power values, the latter expressed in dBm. Equation (3) can be expanded into a second-order Taylor

series around a reference peak power P_{REF} again expressed in dBm. As can be seen in the two examples for peak power values lower (Fitting $1-R^2=0.9989$) and higher (Fitting $2-R^2=0.9949$) than 0 dBm illustrated in Fig. 1(b), the second-order Taylor expansion provides a very good approximation to the curved sections of T_{MEAN} over a power range of more than 15 dB. Moreover, by substituting in (4) the values of T_{MEAN} corresponding to the highest and lowest peak power pulses $P_p^{\max}$ (dBm) and $P_p^{\min}$ (dBm), respectively, the deterministic timing jitter can now be written as

$$J_{pp}^{D}=\frac{1}{2!}a\cdot\left[\left(P_p^{\max}(\mathrm{dBm})-P_{REF}(\mathrm{dBm})\right)^2-\left(P_p^{\min}(\mathrm{dBm})-P_{REF}(\mathrm{dBm})\right)^2\right]+b\cdot\left(P_p^{\max}(\mathrm{dBm})-P_p^{\min}(\mathrm{dBm})\right). \quad (5)$$

where

$$a=\left.\frac{d^2J_{pp}^{D}}{dP^2}\right|_{P=P_{REF}(\mathrm{dBm})} \quad \text{and} \quad b=\left.\frac{dJ_{pp}^{D}}{dP}\right|_{P=P_{REF}(\mathrm{dBm})}.$$

Equation (5) can be further simplified using some straightforward algebra into

$$J_{pp}^{D}=\frac{1}{2!}a\cdot\Delta P(dB)\cdot\left[P_p^{\max}(\mathrm{dBm})+P_p^{\min}(\mathrm{dBm})-2\cdot P_{REF}(\mathrm{dBm})\right]+b\cdot\Delta P(dB) \quad (6)$$

where $\Delta P=P_p^{\max}(\mathrm{dBm})-P_p^{\min}(\mathrm{dBm})$ is the intensity modulation expressed in dB. By selecting the $P_{REF}(\mathrm{dBm})$ value to be the midpoint between the minimum $P_p^{\min}$ and maximum $P_p^{\max}$ peak power levels, so that $P_p^{\max}(\mathrm{dBm})=P_{REF}(\mathrm{dBm})+\Delta P(dB)/2$ and $P_p^{\min}(\mathrm{dBm})=P_{REF}(\mathrm{dBm})-\Delta P(dB)/2$, the quantity contained in the brackets of (6) becomes zero, and the deterministic jitter expression turns into

$$J_{pp}^{D}=b\cdot\Delta P(dB). \quad (7)$$

Factor b is provided by

$$b=-\frac{T_o^2\cdot e^{\frac{P_{REF}(dBm\cdot10^{-3})}{10}}\cdot(G_o-1)\cdot\left(\begin{array}{c}2\cdot G_o-2\cdot G_o\cdot e^{\frac{T_o\cdot\sqrt{\pi}\cdot U_{sat}\cdot e^{\frac{P_{REF}(dBm\cdot10^{-3})}{10}}}{2}}+G_o\cdot T_o\cdot\sqrt{\pi}\\ \cdot U_{sat}\cdot e^{\frac{P_{REF}(\cdot10^{-3})}{10}}+\frac{T_o\cdot\sqrt{\pi}\cdot U_{sat}\cdot e^{\frac{P_{REF}(dBm\cdot10^{-3})}{10}}}{2}-2\end{array}\right)}{40\cdot U_{sat}\cdot\left(G_o\cdot e^{\frac{T_o\sqrt{\pi}U_{sat}e^{\frac{P_{REF}(dBm\cdot10^{-3})}{10}}}{2}}-G_o+1\right)^2}. \quad (8)$$

By selecting a certain value for P_{REF}, factor b turns into a constant, and (7) reveals a linear relationship between deterministic jitter and intensity modulation.

3. Experimental Details

Fig. 2 shows the experimental setup for the deterministic timing jitter measurements with variable pulsewidths and SOA gain levels. It consists of a 1549.2-nm mode-locked laser (TMLL) with typical jitter of 100 fs and a Ti:$LiNbO_3$ electrooptic modulator (MOD) driven by a 10-GHz pattern of alternating "1's" and "0's", to create clock pulses at 5 GHz, so as to ensure a pulse period greater than the SOA gain recovery time (160-ps 1/e). The clock signal is then injected into a second modulator driven by a 625-MHz sinusoidal signal to create intensity-modulated pulses with eight different pulse peak power levels. The intensity-modulated clock signal is then amplified (EDFA) and directed into the SOA. Two SMF spools of 800 m and 1225 m were employed to enable pulsewidth adjustment of 20 ps and 30 ps, respectively, through fiber dispersion. An additional CW at 1555.8 nm was utilized to adjust the SOA gain level and as such to determine its operational regime. The output pulse train was then captured on a real-time oscilloscope (RTO) with 16-GHz

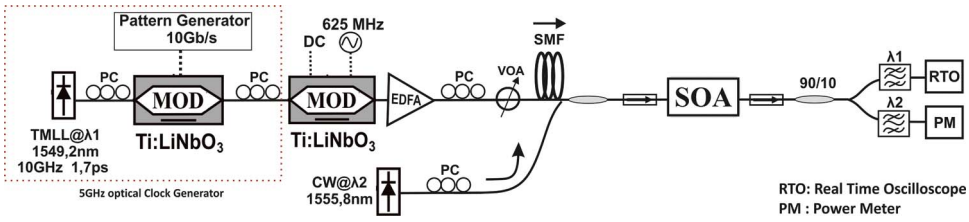

Fig. 2. Experimental setup.

bandwidth, and 300-fs jitter measurement floor for offline postprocessing. The control and input signal were adjusted in terms of power and polarization by means of variable optical attenuators (VOAs) and polarization controllers (PCs). The SOA module was a commercial 1.5-mm-long multiquantum-well structure with 31-dB small signal gain and was driven at 450 mA.

The U_{sat} parameter of SOA was found to be approximately 7 fJ. The jittery pulses captured on the oscilloscope at 100 GSa/s were reconstructed with a sample time resolution of $\Delta t = 1.25$ ps, after eightfold upsampling. For each run, the total output timing jitter, referred to as J^{TOTAL}, was calculated over 8192 pulses by means of (1). J^{TOTAL} is, however, the combination of deterministic and random jitters. In order to obtain experimental results for the deterministic jitter, the stochastic contribution of the noise-induced random jitter has to be separated from the deterministic process that leads to pulse position variations proportional to the pulses' intensity modulation.

To achieve this, the deterministic jitter is represented as a peak-to-peak value (J^D_{pp}) between minimum and maximum values since no probabilistic distribution can be applied, while the random jitter is considered as the peak-to-peak value of a normal distribution (J^R_{pp}). J^{TOTAL} is then approximated by [10], [11]

$$J^{TOTAL} = J^R_{PP} + J^D_{PP}. \tag{9}$$

The total jitter at the output of the SOA in absence of pulse peak power variations is uncorrelated to the jitter induced from an intensity-modulated pulse sequence and actually represents the accumulated random jitter of our experimental system, so that

$$J^R_{PP} = J^{TOTAL}|_{0dB\ AM}. \tag{10}$$

Therefore, the deterministic timing jitter J^D_{pp} is obtained by subtracting the random jitter measurement floor J^R_{pp} from J^{TOTAL} when the input pulse sequence has a given intensity modulation.

4. Results

Table 1 summarizes the timing jitter values at the input and output of the SOA when power-equalized pulses were used as the input signal, for pulsewidth values of 20 ps and 30 ps, and for SOA gains equal to 20 dB and 31 dB, respectively. Fig. 3(a) depicts the eye diagram of a 10-dB intensity-modulated input signal with 20-ps pulsewidth, and Fig. 3(b) is the respective eye diagram for 30-ps pulsewidth. Fig. 3(c) and (d) shows the eye diagrams obtained at the output of the SOA for the two pulsewidths when the SOA operates in the nonsaturated regime. Fig. 3(e) and (f) depicts a similar set of results for the two pulsewidths in the case that SOA operates in the strongly saturated region. The SOA gain level is equal to 20 dB in both cases, and the experimental average peak power values are 30 μW and 1.85 mW for the non saturated and strongly saturated SOAs with 20-ps pulses, and 34 μW and 1.23 mW with 30-ps pulses. Fig. 3(c)–(f) shows the irregular shapes of the output eye diagrams revealing the pulse shape distortion that generates the deterministic timing jitter. Fig. 3(g)–(i) depicts the experimental and theoretical results of the deterministic timing jitter versus input signal intensity modulation expressed in dB, for different gain levels, SOA saturation regimes, and pulsewidths. The theoretical timing jitter curves have been calculated by using (3) and (4).

TABLE 1

Timing jitter values at the input and at the output of the SOA

Pulsewidth	SOA INPUT		Gain	SOA OUTPUT	
	Random Jitter (ps)			Random jitter floor J_{PP}^{R} (ps)	
				Non Saturation	*Saturation*
20 ps	J_{RMS}^{R}	0.585	20 dB	4.356	4.391
30 ps		0.634		5.065	5.180
20 ps	J_{PP}^{R}	4.048	31 dB	6.082	4.223
30 ps		4.460		6.596	5.779

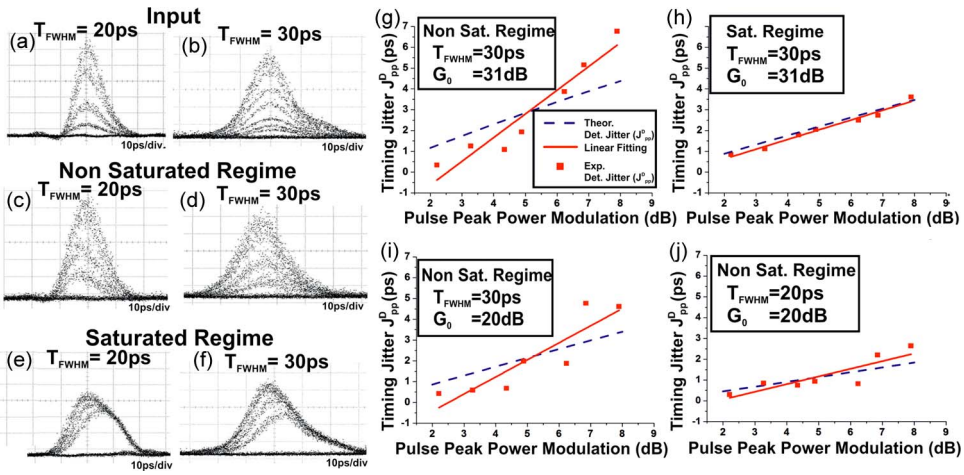

Fig. 3. (a), (b) Eye diagram of a SOA input signal with 10 dB intensity modulation (a) at 20 ps and (b) 30 ps, and (b), (c) respective SOA output when operating in the nonsaturated and (e), (f) strongly saturated regimes with SOA gain equal to 20 dB. Time scale for (a)–(f): 10 ps/div. Experimental and theoretical results for deterministic timing jitter versus pulse intensity modulation expressed in dB with 30 ps long pulses with 31 dB SOA gain for (g) nonsaturated, (h) strongly saturated regimes and for 20-dB SOA gain and nonsaturated regime with (i) 30-ps and (j) 20-ps pulsewidths, respectively.

Since (7) reveals an approximate linear dependence of theoretical deterministic jitter for intensity modulation levels, a linear fit was also applied to the experimental data showing that close agreement between theory and experiment is obtained for all cases. Fig. 3(g) and (h) depicts theoretical jitter results obtained by applying (4), as well as the experimental data with their linear fit for 30-ps pulsewidth and 31-dB SOA gain level, using average pulse peak power values of 11 μW and 235 μW for unsaturated and saturated SOA operations, respectively. The graphs reveal a reduction of deterministic jitter in excess of 25% for the case of the saturated regime compared with the nonsaturated regime. Fig. 3(i) illustrates jitter evolution versus intensity modulation levels for 20-dB SOA gain using an average pulse peak power value of 34 μW. When compared with Fig. 3(g), a decrease of jitter with the SOA gain level is evident. Finally, Fig. 3(i) and (j) depicts the jitter results for 30-ps and 20-ps pulsewidths, respectively, when all other operating parameters are the same, confirming that shorter pulses generate lower jitter levels [30-μW average pulse peak power value for Fig. 3(j)]. The R^2 values for the linear fits applied to the experimental data in Fig. 3(g) and (i) were 0.87 and 0.79, respectively, while for Fig. 3(h) and (j), both linear fits exhibit an improved matching with R^2 values higher than 0.98.

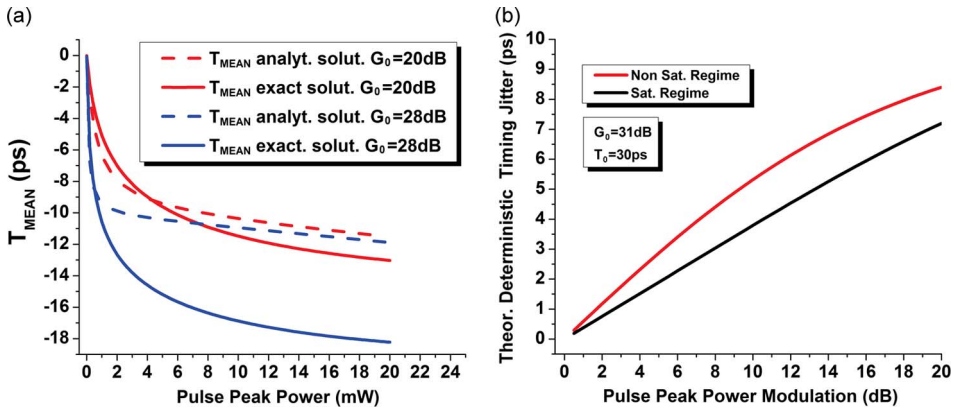

Fig. 4. (a) Mean arrival time T_{MEAN} calculated by means of (2) (exact solution, solid line) and (3) (analytical solution, dashed line) for two different SOA steady-state gain values, i.e., 20 dB (red lines) and 28 dB (blue lines). (b) Deterministic timing jitter calculated theoretically through (3) and (4) over an intensity modulation range from 0 to 20 dB for a pulsewidth of 30 ps and a SOA steady-state gain of 31 dB.

5. Discussion

The main approximation made toward calculating the mean arrival time expression provided by (3), which has been subsequently used for calculating theoretically the deterministic timing jitter curves shown in Fig. 3(g)–(j), relied on the first-order Taylor expansion of the SOA gain $G(t)$ around the pulse center at $t = 0$. Fig. 4(a) depicts the mean arrival time values calculated for two SOA steady-state gain values both by the analytical formula provided by (3) and by the original relationship provided by (2), i.e., before any approximation was applied, in order to address the validity of our approximation. In the case of 28-dB steady-state gain, the two respective curves are almost identical for a power range from 0 to 1 mW. After this value, the analytic solution starts immediately to approach asymptotically a minimum value, while the exact solution continues to decrease smoothly until a pulse peak power value of 4 mW and then starts also to follow an asymptotic behavior. As such, the two curves experience a very good quantitative matching until 1 mW and then show a good qualitative agreement in their performance, which is very important for timing jitter calculation since it relies on the difference between the mean arrival times and not on their exact absolute values. When the SOA steady-state gain is lowered down to 20 dB, the two curves are almost the same over the complete power range from 0 to 20 mW, providing also very good quantitative matching with the highest deviation being only 1 ps at pulse peak power levels higher than 12 mW. The main reason for the improved matching between the exact solution and the approximated solution provided by (3) lies in the way the gain depletes. The Taylor expansion of the $G(t)$ gain expression around $t = 0$ (i.e., the center of the pulse) means that we consider the gain depletion to follow a linear curve around $t = 0$. This is indeed true for the case of $G_o = 20$ dB, but the linearity at $t = 0$ starts to degrade for higher steady-state gain values and for the same pulse peak power level due to the faster gain depletion mechanism in this case.

The validity of the mathematical framework concluding to (7) for the linear dependence of the deterministic timing jitter on the intensity modulation can be estimated by means of Fig. 4(b). It shows the deterministic timing jitter calculated by means of (3) and (4) over an intensity modulation range from 0 up to 20 dB, i.e., a significantly higher range than 8 dB shown in Fig. 3(g)–(j). As can be noticed from this graph, in the nonsaturated operational regime of the SOA, the jitter curve is not linear across all this range, but it can be very well approximated as linear up to an intensity modulation value of 8–10 dB. In the case of SOA operation in its saturated regime, the timing jitter curve is almost linear over the entire intensity modulation range. To this end, (7) can be indeed perceived as a solid mathematical formula for demonstrating the linearity between deterministic timing jitter and intensity modulation for practical intensity modulation levels up to 10 dB.

The pulse waveform that has been used throughout our complete theoretical and experimental analysis relied on a Gaussian-type distribution. It should be noted that our theoretical framework for deterministic timing jitter calculation can be also applied to any other type of optical pulse shapes by simply replacing the expression $\exp(-t^2/T_o^2)$ in (2) with the new mathematical formula describing a different pulse waveform. However, as this has been the first ever reported attempt to theoretically predict the deterministic timing jitter induced by SOAs in the case of intensity-modulated pulses, our main goal has been to demonstrate for the first time the quantitative and qualitative behaviors of SOA-induced deterministic jitter with an extensive analysis for several pulse waveforms falling beyond the scope of this paper. In this first attempt, the main reasons for utilizing Gaussian-type pulses have been the simplicity offered by Gaussian-type distributions in their mathematical treatment, the experimentally confirmed Gaussian waveform of short optical pulses with up to 20-ps pulsewidth usually generated by optical laser sources [12]–[14], and their extensive use in theoretical approaches applied in SOA devices [6], [15]–[19].

The theoretical analysis presented can be also extended toward calculating the deterministic jitter in the case of random data patterns with intensity-modulated pulses used as the input signal in SOAs. As long as the SOA gain recovery time is shorter than the bit period, all data pulses will again experience the same steady-state gain G_o, rendering (3) valid also for this case. But even when the SOA gain recovery time is longer than the bit period, (3) serves as a good basis for calculating the mean arrival time T_{MEAN} of the data pulses and, subsequently, the deterministic timing jitter J_{pp}^D. In this case, the use of random data pattern will actually result in different gain levels perceived by every individual pulse. To this end, the assumption that every pulse experiences the same steady-state gain value G_o is not any more valid, but G_o should be now treated as an additional variable in (3) taking values within a certain range ΔG_o.

This actually turns relationship (3) into a two-variable function, assuming a given pulsewidth and a constant U_{sat} parameter. As can be also noticed in Fig. 1, the same pulse peak power level results to a lower absolute value for the pulse mean arrival time when a lower gain value is perceived by the pulse. In Fig. 1, for example, the absolute value of T_{MEAN} for a gain of 20 dB is always smaller than the respective value for a SOA gain of 28 dB, which, in turn, is always smaller than the respective value for a 30-dB gain. This actually means that the deterministic jitter in case of different gain levels perceived by every pulse, as will be the case with random data patterns and gain recovery times longer than the bit period, will be always slightly higher than the deterministic jitter induced by the same pulse sequence when the SOA gain recovery time is shorter than the bit period. This can be easier understood by considering the following example: the data pulse with the smallest peak power level comes after a long sequence of "1's", experiencing in this way the smallest SOA gain among all data pulses and yielding the smallest absolute value for its mean arrival time at the SOA output. At the same time, the highest data pulse comes after a long sequence of "0's", so that it actually perceives the full gain of the amplifier, resulting to the highest absolute value among all data pulses for its mean arrival time T_{MEAN}. This scenario can be certainly met when considering a truly random data pattern with a uniform or Gaussian statistical distribution of pulse intensity modulation. As such, (3) indicates that higher deterministic jitter values are expected; however, the exact analysis of this case falls beyond the scope of this paper.

At this point, it should be also noted that using an external CW signal instead of altering the SOA driving current for controlling the SOA gain operational regime does not impact the validity of our conclusions. The equation of the SOA gain $G(t)$ [6] can be successfully applied even when the steady-state gain G_o is different than the SOA small-signal gain [20]. The SOA gain control could have been also certainly obtained by controlling the SOA driving current, but in that case, the SOA gain recovery time would increase significantly with reduced driving current values, rendering the condition of our analysis for SOA gain recovery times lower than the pulse period as invalid in our experiment. On the other hand, gain control by means of an external CW signal allows also for further reductions in the SOA gain recovery time values [21], ensuring that our condition is fulfilled in all our measurements and for all SOA gain levels being investigated.

6. Conclusion

We have demonstrated a theoretical and experimental analysis of the deterministic timing jitter induced on intensity-modulated optical pulse streams when amplified in a SOA. The theoretical timing jitter model relies on the calculation of the pulse mean arrival time as a function of the pulse peak power, the pulsewidth, and the SOA steady-state gain. Both experimental and theoretical results reveal an approximate linear relationship of deterministic timing jitter versus intensity modulation levels up to 8 dB when the SOA gain recovery time is shorter than the pulse period. Nonsaturated SOA operation and higher SOA gain yield higher deterministic timing jitter values.

References

[1] L. Aggazi, J. D. B. Bradley, M. Dijkstra, F. Ay, G. Roelkens, R. Baets, K. Wörhoff, and M. Pollnau, "Monolithic integration of the erbium-doped amplifier with silicon-on-insulator waveguides," *Opt. Exp.*, vol. 18, no. 26, pp. 27703–27711, Dec. 2010.

[2] C. S. Nicholes, M. L. Mašanovi, B. Jevremovi, L. A. Coldren, and D. J. Blumenthal, "An 8 × 8 InP monolithic tunable optical router (MOTOR) packet forwarding chip," *J. Lightw. Technol.*, vol. 28, no. 4, pp. 641–650, Feb. 2010.

[3] V. S. Pato, R. Meleiro, D. Fonseca, P. Andre, P. Monteiro, and H. Silva, "All-optical burst mode power equalizer based on cascaded SOAs for 10-Gb/s EPONs," *Photon. Tech. Lett.*, vol. 20, no. 24, pp. 2078–2080, Dec. 2008.

[4] D. Chiaroni, C. Simonneau, M. Salsi, G. Buforn, S. Etienne, H. Mardoyan, J. E. Simsarian, and J.-C. Antona, "Optical packet ring network offering bit rate and modulation formats transparency," presented at the OFC/NFOEC, San Diego, CA, 2010, OWI3.

[5] R. Bonk, G. Huber, T. Vallaitis, R. Schmogrow, D. Hillerkuss, C. Koos, W. Freude, and J. Leuthold, "Impact of alfa-factor on SOA dynamic range for 20 GBd BPSK, QPSK and 16-QAM signals," presented at the OFC/NFOEC, Los Angeles, CA, 2011, OML4.

[6] G. P. Agrawal and N. A. Olsson, "Self-phase modulation and spectral broadening of optical pulses in semiconductor laser amplifiers," *J. Quantum Electron*, vol. 25, no. 11, pp. 2297–2306, Nov. 1989.

[7] T. Alexoudi, S. Dris, D. Kalavrouziotis, P. Bakopoulos, A. Miliou, and N. Pleros, "Timing jitter of SOA-amplified intensity modulated optical pulses," presented at the National Fiber Optic Eng. Conf. (NFOEC), Los Angeles, CA, Mar. 4, 2012, JTh2A.

[8] S. V. Kartalopoulos, *Optical Bit Error Rate: An Estimation Methodology,* 1st ed. Hoboken, NJ: Willey, 2004.

[9] J. Peatross, S. A. Glasgow, and M. Ware, "Average energy flow of optical pulses in dispersive media," *Phys. Rev. Lett.*, vol. 84, no. 11, pp. 2370–2373, Mar. 2000.

[10] *Measuring Jitter in Digital Systems*, Agilent Technol., Santa Clara, CA, 2006, Appl. Note 1448-1. [Online]. Available: http://cp.literature.agilent.com/litweb/pdf/5988-9109EN.pdf

[11] *Converting Between RMS to Peak-to-Peak Jitter at a Specified BER*, Maxim Integr., San Jose, CA, 2008, Appl. Note 462 HFAN-04.0.2. [Online]. Available: http://www.maxim-ic.com/app-notes/index.mvp/id/462

[12] J. Peng, L. Zhan, Z. Gu, K. Qian, S. Luo, and Q. Shen, "Direct generation of 128-fs Gaussian pulses from a compensation-free fiber laser using dual mode-locking mechanisms," *Opt. Commun.*, vol. 285, no. 5, pp. 731–733, Mar. 1, 2012.

[13] Q. Wang, F. Zeng, S. Blais, and J. Yao, "Optical ultrawideband monocycle pulse generation based on cross-gain modulation in a semiconductor optical amplifier," *Opt. Lett.*, vol. 31, no. 21, pp. 3083–3085, Nov. 2006.

[14] J. P. van der Ziel, H. Temkin, R. D. Dupuis, and R. M. Mikulyak, "Mode-locked picosecond pulse generation from high power phase-locked GaAs laser arrays," *Appl. Phys. Lett.*, vol. 44, no. 4, pp. 357–359, Nov. 1984.

[15] A. Abd El Aziz, W. P. Ng, Z. Ghassemlooy, M. H. Aly, and R. Ngah, "SOA gain uniformity improvement employing a non-uniform biasing technique for ultra-high speed optical routers," in *Proc. 7th Int. Symp. CSNDSP*, Jul. 2010, pp. 642–647.

[16] A. Reale, A. Di Carlo, and P. Lugli, "Gain dynamics in traveling-wave semiconductor optical amplifiers," *IEEE J. Sel. Topics Quantum Electron.*, vol. 7, no. 2, pp. 293–299, Mar./Apr. 2001.

[17] M. Premaratne, D. Neši, and G. P. Agrawal, "Pulse amplification and gain recovery in semiconductor optical amplifiers: A systematic analytical approach," *J. Lightw. Technol.*, vol. 26, no. 12, pp. 1653–1660, Jun. 2008.

[18] P. P. Baveja, D. N. Maywar, A. M. Kaplan, and G. P. Agrawal, "Self-phase modulation in semiconductor optical amplifiers: Impact of amplified spontaneous emission," *IEEE J. Quantum. Electron.*, vol. 46, no. 9, pp. 1396–1403, Sep. 2010.

[19] G. P. Agrawal, "Effect of gain dispersion on ultrashort pulse amplification in semiconductor laser amplifiers," *IEEE J. Quantum. Electron.*, vol. 27, no. 6, pp. 1843–1849, Jun. 1991.

[20] N. Pleros, C. Bintjas, G. T. Kanellos, K. Vlachos, H. Avramopoulos, and G. Guekos, "Recipe for intensity modulation reduction in SOA-based interferometric switches," *J. Lightw. Technol.*, vol. 22, no. 12, pp. 2834–2841, Dec. 2004.

[21] R. J. Manning and D. A. O. Davies, "Three-wavelength device for all-optical signal processing," *Opt. Lett.*, vol. 19, no. 12, pp. 889–991, Jun. 1994.